Entanglement Tension and Brane Secession: A Holographic Framework for Emergent Gravity and Mass

César Henriques
cesar@mobisoft.com.ar

February 7, 2026

Contents

Abstract

We present a holographic framework in which four-dimensional spacetime emerges from quantum entanglement structure encoded on a brane embedded in asymptotically AdS space [1]. Mass is not fundamental but is identified with topological entanglement complexity—knot complexity C_k—quantifying irreducible multipartite correlations [3]. Gravitational interaction emerges as the macroscopic response to gradients in entanglement tension along the holographic direction [4], reducing to Einstein's equations at low complexity with an additional non-local stress contribution from diffuse entanglement structure [5].

We propose that classical spacetime singularities signal saturation of entanglement capacity at a critical threshold $C_{k,\max}$, analogous to the Bekenstein–Hawking bound [6, 7]. Beyond this regime, the system undergoes a topological transition—brane secession—whereby the saturated region disconnects from the parent structure and nucleates an independent spacetime [2, 8]. This provides a natural regularization mechanism: from the exterior perspective, a black hole forms; from the interior perspective, a smooth cosmological expansion emerges, unifying collapse and cosmogenesis as dual descriptions of a single entanglement reorganization.

We demonstrate structural consistency through explicit toy-model calculations in finite tensor networks (Appendices A–B) and present a simplified phenomenological realization showing how diffuse entanglement tension reproduces flat galactic rotation curves without dark matter particles (Section 5.3). The framework offers a unified interpretive scheme for mass, gravity, and dark-sector phenomenology as emergent consequences of quantum correlation structure, while remaining compatible with established results in holography, semiclassical gravity, and observational cosmology [1, 2, 6].

1 Introduction

General Relativity (GR) remains one of the most successful physical theories, providing an extraordinarily accurate description of gravitational dynamics at macroscopic scales [5]. Nevertheless, its classical formulation inevitably predicts spacetime singularities, notably within black hole interiors and at the origin of cosmological expansion, where physical quantities diverge and the geometric description ceases to be predictive [6]. This long-standing issue strongly suggests that spacetime geometry is not a fundamental entity, but rather an effective macroscopic manifestation of deeper microscopic degrees of freedom [3].

Over the past decades, significant progress in quantum gravity has reinforced this perspective. The AdS/CFT correspondence [1] has provided a concrete realization of the holographic principle, demonstrating that gravitational dynamics in a higher-dimensional bulk spacetime can be encoded in a lower-dimensional quantum field theory. Complementarily, the ER=EPR conjecture [2, 10] has established a direct conceptual link between spacetime connectivity and quantum entanglement, implying that geometric structure itself may emerge from patterns of entanglement. In this view, spacetime ceases to be a primitive construct and instead arises as an organizational feature of quantum information [3, 11].

Motivated by these insights, this work proposes a holographic framework in which a four-dimensional effective spacetime emerges as a brane ($\mathcal{B}_H$) embedded in a five-dimensional asymptotically Anti-de Sitter (AdS) bulk [1, 9]. The fundamental degrees of

freedom are not geometric, but informational, organized as networks of quantum entanglement [3, 11]. Within this framework, mass is not treated as an intrinsic property of matter, but as a measure of topological entanglement complexity, hereafter referred to as knot complexity C_k [3, 7]. Regions of high C_k correspond to dense, stable nodes in the entanglement network, while low-complexity regions appear macroscopically as vacuum.

A central assumption of the model is that, prior to gravitational collapse, the entanglement-induced tension associated with massive structures is directed predominantly along the holographic (bulk) dimension [4]. Extended objects such as galaxies are thus interpreted as open, metastable configurations whose entanglement links remain anchored to a higher-dimensional progenitor structure, referred to as the parent brane [9]. In this regime, gravitational attraction does not arise from local self-curvature alone, but from the redistribution of entanglement pathways that minimize informational tension toward the parent structure [4]. This perspective reframes gravitational attraction as a collective optimization process rather than as a fundamental force.

Gravitational collapse occurs when the local entanglement complexity saturates a critical bound, analogous to the Bekenstein–Hawking entropy limit [6, 7]. At this point, entanglement pathways can no longer be redistributed along the holographic direction, leading to a topological closure of the network [3]. This transition defines the formation of a black hole horizon, interpreted here not as a geometric singularity but as an interface of maximal entanglement [6]. Crucially, the breakdown of classical geometry is avoided: instead of a singularity, the model predicts a topological phase transition termed *brane secession*, whereby the saturated entanglement structure disconnects from the parent brane and gives rise to a new emergent spacetime region [2, 8].

From the perspective of the parent brane, this process manifests as the formation and growth of a conventional black hole, complete with Hawking radiation and semiclassical gravitational behavior [6]. From the complementary perspective of the newly generated brane, the same transition is experienced as a cosmological expansion originating from a smooth initial surface, effectively replacing the Big Bang singularity with a boundary-driven emergence of spacetime [2, 8]. In this sense, black hole interiors and cosmological origins are unified as dual descriptions of a single holographic transition.

2 Conceptual Framework and Axiomatic Structure

2.1 Emergent Spacetime and Holographic Embedding

Axiom 2.1 (Holographic Emergence of Spacetime)**.** *Four-dimensional spacetime is not fundamental. It emerges as an effective description of an underlying network of quantum entanglement encoded on a brane $\mathcal{B}_H$ embedded in a five-dimensional asymptotically AdS bulk [1, 9].*

In this picture, spacetime geometry arises as a coarse-grained manifestation of informational degrees of freedom [3]. Local distances and curvature correspond to the density and organization of entanglement links within the network. The bulk coordinate plays the role of a holographic scale, encoding entanglement depth or coarse-graining level rather than a conventional spacetime dimension [4, 5, 11].

2.2 Entanglement Threads and Effective Tension

The fundamental microscopic entities in this framework are *entanglement threads*: abstract, nonlocal connections encoding quantum correlations across the brane and into the bulk [2, 3]. These threads are characterized by an effective resistance to reconfiguration, referred to as *entanglement tension* [4].

Entanglement tension should be understood as a coarse-grained, emergent quantity analogous to entropic forces, rather than as a fundamental local observable or a string-theoretic tension [4]. It quantifies the energetic and informational cost of deforming the entanglement network under coarse-graining. Similar notions arise in tensor-network models of holography and entanglement-based reconstructions of geometry [3, 4, 11, 12].

Regions of concentrated entanglement tension form stable configurations, hereafter referred to as *tension knots*. These knots act as persistent sources of geometric deformation in the emergent spacetime [3].

2.3 Knot Complexity and the Nature of Mass

Axiom 2.2 (Mass–Complexity Equivalence)**.** *Mass is an emergent, topological quantity proportional to knot complexity:*

$$M = \alpha\, C_k, \tag{1}$$

where C_k measures irreducible multipartite entanglement within a coarse-grained region and α sets the physical scale [3, 7].

While no unique microscopic definition of C_k is assumed, it may be understood as a quantity related to tensor-network minimal cuts, topological entanglement entropy, or circuit complexity [3, 7, 13]. Inertia arises as the resistance of such entanglement knots to reconfiguration [4].

Formal characterization. At the effective level, C_k is defined as a coarse-grained scalar functional of the reduced density matrix $\rho_{\mathcal{R}}$ of a spatial region $\mathcal{R}$, capturing only topologically stable, non-local entanglement structures that survive renormalization-group flow. Contributions from local unitary transformations and short-range entanglement are explicitly excluded.

Operationally, C_k may be associated with the minimal preparation complexity of $\rho_{\mathcal{R}}$ from a disentangled reference state, or equivalently with the minimal number of nontrivial entanglement links crossing an effective tensor-network cut homologous to $\mathcal{R}$ [11, 12, 13]. This definition ensures that C_k behaves as an extensive, positive quantity and vanishes in the absence of irreducible entanglement.

2.4 Gravitation as Entanglement Tension

Axiom 2.3 (Emergent Gravitation)**.** *Gravitational interaction arises as the macroscopic response of the emergent brane $\mathcal{B}_H$ to gradients in entanglement tension along the holographic direction [4, 5].*

Prior to collapse, this tension is predominantly directed toward the parent structure [9]. Gravitational attraction between massive objects reflects a collective reorganization of entanglement pathways that minimizes global tension, rather than a fundamental interaction propagating on a fixed background [4].

Effective description. Entanglement tension is modeled as an emergent response to spatial variations of knot complexity. At the continuum level, this response is encoded in an effective stress-energy contribution $T_{\mu\nu}^{(\tau)}$, which supplements ordinary matter sources in the gravitational field equations. The resulting dynamics recover General Relativity in the limit of homogeneous or vanishing C_k, while allowing for additional gravitational effects sourced by entanglement structure alone.

2.5 Saturation, Horizons, and Brane Secession

Axiom 2.4 (Entanglement Saturation)**.** *There exists a critical entanglement complexity $C_{k,\max}$, analogous to the Bekenstein–Hawking entropy bound [6, 7]. When this bound is reached, the entanglement network undergoes a topological transition [3].*

This transition defines horizon formation as a surface of maximal entanglement [6]. Beyond this point, the system avoids singular behavior through *brane secession*: the saturated region disconnects and reorganizes into a new holographic branch [2, 8].

Interpretation. Entanglement saturation represents a breakdown of further coarse-grained reconfiguration within the parent holographic structure. Brane secession is therefore not a dynamical instability but a topological reorganization that preserves unitarity while preventing divergent local complexity.

2.6 Dual Interpretation of Collapse and Expansion

Collapse and expansion are dual manifestations of the same entanglement transition [2, 10]. From the parent perspective, brane secession appears as black hole formation [6]. From the child perspective, it manifests as a smooth cosmological origin characterized by rapid expansion, consistent with holographic complementarity [2, 8, 14].

2.7 Holographic Structure and Brane Hierarchy

Clarification of the Multi-Layer Architecture The framework involves three conceptually distinct structures whose relationship must be carefully specified to avoid confusion.

The Parent Brane ($\mathcal{B}_{\text{parent}}$): This represents the pre-existing holographic structure in which ordinary matter (stars, galaxies, baryonic gas) resides prior to gravitational collapse. It is not itself a fundamental entity but an effective coarse-grained description of an underlying quantum state. The parent brane is characterized by open entanglement pathways: massive objects within it maintain non-local quantum correlations that extend into a higher-dimensional embedding space [9].

The Effective Holographic Screen ($\mathcal{B}_H$): This is the dynamically emergent boundary surface encoding the entanglement structure of the parent brane. It plays the role of a holographic screen in the sense of 't Hooft and Susskind [9], serving as the locus where gravitational degrees of freedom are encoded. Distances and curvature on $\mathcal{B}_H$ correspond to patterns of entanglement connectivity. In the regime where $C_k \ll C_{k,\max}$, $\mathcal{B}_H$ admits a smooth geometric description governed by Einstein's equations.

The Child Bulk ($\mathbf{AdS_{child}}$): Following brane secession, the saturated entanglement region reorganizes into a new holographic branch with its own emergent bulk geometry. This child structure is not assumed but arises dynamically as a consequence of topological closure [2, 8]. The radial AdS coordinate z in the child bulk parametrizes entanglement depth or renormalization scale, not physical distance in the parent frame. Cosmological time within the child brane emerges as a relational variable associated with the progressive unfolding of entanglement structure during post-secession relaxation.

Relationship and Transitions: In the pre-collapse regime:

$$\mathcal{B}_{\text{parent}} \supset \mathcal{B}_H \quad \text{(holographic screen encoding parent state)} \tag{2}$$

At critical saturation:

$$C_k \to C_{k,\max} \quad \Longrightarrow \quad \text{Topological transition (brane secession)} \tag{3}$$

In the post-collapse regime:

$$\mathcal{B}_{\text{parent}} \supset [\text{Horizon}] \supset \text{AdS}_{\text{child}} \supset \mathcal{B}_{\text{child}} \tag{4}$$

The horizon represents the interface of maximal entanglement separating the two holographic branches. Observers on $\mathcal{B}_{\text{parent}}$ perceive black hole formation; observers on $\mathcal{B}_{\text{child}}$ experience smooth cosmological emergence. This duality is enforced by holographic complementarity [2, 14]: the two descriptions are informationally equivalent but operationally disjoint, as no signal crosses the horizon in both directions simultaneously.

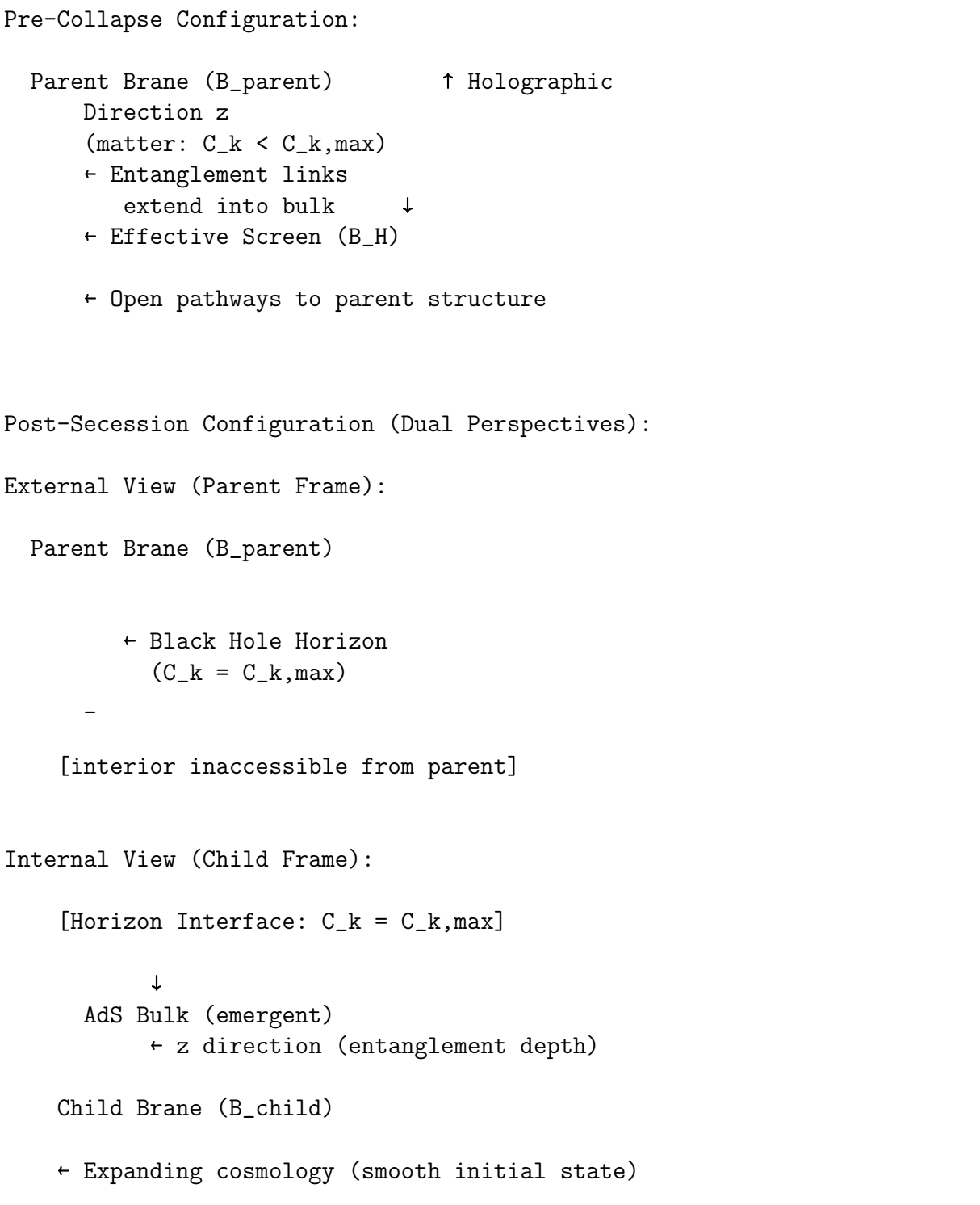

Figure 1: Holographic Architecture: Pre-collapse and post-secession configurations showing parent brane, effective holographic screen, and child bulk structures.

This architecture ensures that singularities never form within any single reference frame. The parent observer sees standard black hole thermodynamics; the child observer experiences smooth cosmological expansion. Both descriptions are complete within their respective holographic domains but cannot be simultaneously accessed [14].

3 Entanglement Tension and Black Hole Birth

3.1 Emergence of the AdS Bulk

The AdS bulk is not assumed as a background but emerges dynamically from post-secession entanglement reorganization. The holographic coordinate z parametrizes entanglement depth rather than time. Cosmological time on the emergent brane arises as a relational parameter associated with dynamical reconfiguration of correlations, not from the bulk coordinate itself.

3.2 Effective Gravity from Entanglement Stress

Localized increases in knot complexity generate gradients in entanglement tension, deforming the effective brane geometry. In the weak-tension regime, this reduces to Einstein gravity as an effective macroscopic description.

3.3 Critical Rupture and Child Black Hole Formation

3.3.1 Accumulation of Knots

Galactic mergers and accretion increase local knot density, raising entanglement tension without inducing collapse.

3.3.2 Critical Threshold

When a critical tension T_c is exceeded, the entanglement network undergoes topological rupture.

3.3.3 Dual Interpretation

Externally, this appears as black hole formation. Internally, it corresponds to the nucleation of a new AdS bulk and expanding dS brane.

3.3.4 No Fundamental Strings

Entanglement links are not physical strings but effective correlations, akin to ER bridges or tensor-network connections [10, 12].

4 Phenomenology and Consistency with Known Physics

In this section we examine the phenomenological implications of the proposed framework and its consistency with established results in General Relativity, cosmology, and holographic duality. While the model is primarily conceptual and does not yet provide detailed numerical predictions, it admits well-defined limiting regimes in which known physics is recovered. At the same time, it offers alternative interpretations for dark matter, dark energy, and black hole thermodynamics as emergent effects of entanglement structure rather than as fundamental inputs.

4.1 Weak-Field Limit and Emergence of General Relativity

In regions where the entanglement complexity C_k remains well below the critical saturation threshold $C_{k,\max}$, entanglement knots are sparse and the associated tension gradients vary smoothly over macroscopic scales. In this low-complexity regime, the embedding of the effective four-dimensional brane $\mathcal{B}_H$ into the bulk is weakly deformed, and the informational stress induced by entanglement tension admits a local, coarse-grained description.

Under these conditions, the response of the brane geometry to entanglement tension can be encoded in an effective metric satisfying Einstein-like field equations. General Relativity therefore emerges as the long-wavelength, low-tension limit of the underlying informational dynamics, ensuring consistency with all experimentally tested gravitational phenomena.

4.2 Galactic Scales and Effective Dark Matter Phenomenology

At galactic and sub-galactic scales, matter concentrations correspond to localized regions of elevated knot complexity embedded within an extended network of entanglement links. These links do not decay sharply outside regions of visible matter, resulting in nonlocal contributions to the effective gravitational response.

Test particles moving within such regions respond to the cumulative entanglement tension field rather than solely to baryonic mass distributions. This mechanism naturally reproduces qualitative features commonly attributed to dark matter, such as flat galactic rotation curves and enhanced gravitational binding, without introducing additional particle species. In this interpretation, dark matter emerges as a geometric effect of extended entanglement structure rather than as a new form of matter.

Discriminating this framework from MOND and particle dark matter: A key observational distinction lies in gravitational lensing. In modified gravity theories such as MOND, lensing and dynamical effects are directly coupled through the modified acceleration scale. In particle dark matter models, lensing traces the dark matter density profile. In the present framework, gravitational lensing is sourced by the effective stress-energy tensor $T^{(\tau)}_{\mu\nu}$, which encodes the spatial distribution of entanglement complexity gradients. This predicts potential mismatches between lensing mass maps and both baryonic distributions and rotation curve fits in regions where entanglement structure has non-trivial topology—such as in merging systems or filamentary large-scale structures. Detailed lensing surveys combined with high-resolution rotation curve measurements in diverse galactic environments could provide discriminating tests [17, 18].

4.3 Cosmological Expansion and Effective Dark Energy

Following a brane secession event, the emergent four-dimensional brane undergoes large-scale expansion driven by the global reconfiguration and gradual stretching of entanglement links. As the brane separates from the saturation interface, entanglement tension becomes approximately homogeneous across cosmological scales.

This homogeneous tension manifests as an effective negative pressure acting on the brane geometry, leading to accelerated expansion analogous to that attributed to dark energy. Importantly, this effect is not associated with a fundamental cosmological constant, but arises dynamically from the relaxation of the post-secession entanglement network.

4.4 Black Hole Thermodynamics and Information Preservation

Within this framework, black hole thermodynamics arises directly from the statistical properties of entanglement links. The Bekenstein–Hawking entropy corresponds to the maximal density of active entanglement connections that can be supported without triggering topological rupture. The area-law scaling of entropy reflects the saturation of entanglement capacity at the horizon interface.

Hawking radiation is interpreted as thermal fluctuations of near-critical entanglement links at the saturation boundary. As the system approaches the critical tension threshold, these fluctuations give rise to information leakage consistent with semiclassical expectations. The onset of brane secession prevents the formation of curvature singularities, ensuring that information is reorganized into a new holographic branch rather than destroyed [14, 15].

4.5 Observational Outlook and Falsifiability

Although the present work does not derive precise quantitative predictions, the framework suggests several qualitative avenues for observational testing. These include deviations from purely local gravitational behavior in low-acceleration regimes, correlations between galactic-scale dynamics and large-scale cosmological expansion, and potential links between black hole mass growth and surrounding spacetime response beyond classical expectations.

Such features provide pathways for falsification as observational precision improves, distinguishing entanglement-based emergent gravity scenarios from standard ΛCDM cosmology.

Section 4 Summary The proposed framework reproduces known gravitational and cosmological behavior in appropriate limits while offering a unified interpretation of dark matter, dark energy, and black hole singularity resolution as emergent phenomena. Although speculative, it remains internally consistent and firmly grounded in established holographic principles.

5 Toward a Complete Theory

5.1 Missing Mathematical Structure

At present, the framework is formulated at a semi-phenomenological level. While the physical interpretation of entanglement tension and topological knot formation is well defined, a fully explicit microscopic action remains to be constructed.

In particular, a complete formulation would require:

- A precise definition of the entanglement tension field $\tau(x)$ as an emergent, coarse-grained quantity.
- An effective stress-energy contribution $T^{(\tau)}_{\mu\nu}$ derived from underlying entanglement degrees of freedom.
- A consistent variational principle compatible with General Relativity in the weak-field limit.

Crucially, the framework does not attempt to replace Einstein gravity, but rather to extend its source sector beyond localized matter fields.

5.2 Relation to Einstein Equations

At macroscopic scales, the effective dynamics are assumed to be governed by modified Einstein equations of the form:

$$G_{\mu\nu} = 8\pi G \left(T_{\mu\nu}^{(\text{matter})} + T_{\mu\nu}^{(\tau)} \right) \tag{5}$$

Here:

- $T_{\mu\nu}^{(\text{matter})}$ arises from topologically stable entanglement knots that survive coarse-graining and behave as localized matter.
- $T_{\mu\nu}^{(\tau)}$ encodes diffuse, nonlocal entanglement tension that does not collapse into particle-like excitations.

This preserves the geometric interpretation of gravity while allowing for gravitational effects without associated luminous matter, naturally accommodating dark matter phenomenology.

5.3 Simplified Phenomenological Example

To illustrate how diffuse entanglement tension reproduces dark-matter-like phenomenology, we present a minimal toy realization with an explicit functional form for $T_{\mu\nu}^{(\tau)}$.

5.3.1 Ansatz for Entanglement Stress-Energy

We model the effective stress tensor sourced by entanglement tension gradients as:

$$T_{\mu\nu}^{(\tau)} = \beta \left[\nabla_\mu C_k \nabla_\nu C_k - \frac{1}{2} g_{\mu\nu} (\nabla C_k)^2 \right] + \gamma g_{\mu\nu} C_k^2 \tag{6}$$

where:

- β is a coupling constant with dimensions [length^2]
- γ is a self-interaction parameter with dimensions [length^{-2}]
- The first term has the structure of a scalar field kinetic stress tensor
- The second term represents effective pressure from knot density

This form is motivated by analogy with scalar field theories coupled non-minimally to gravity and ensures that $T_{\mu\nu}^{(\tau)}$ satisfies the dominant energy condition for appropriate parameter choices [19, 20].

5.3.2 Spherically Symmetric Configuration

Consider a static, spherically symmetric distribution with:

$$C_k(r) = C_0 \exp(-r/r_0) \tag{7}$$

where C_0 is the central complexity and r_0 is a characteristic scale. This profile represents a localized knot (the galactic core) surrounded by exponentially decaying entanglement links extending into the halo region.

The effective metric in the weak-field limit takes the form:

$$ds^2 = -(1 + 2\Phi)dt^2 + (1 - 2\Phi)(dr^2 + r^2 d\Omega^2) \tag{8}$$

where $\Phi(r)$ is the Newtonian-like potential sourced by both matter and entanglement tension.

Solving the linearized Einstein equation $G_{00} \approx 8\pi G(T_{00}^{(\text{matter})} + T_{00}^{(\tau)})$ gives:

$$\Phi(r) = \Phi_{\text{matter}}(r) + \Phi_\tau(r) \tag{9}$$

with the entanglement contribution:

$$\begin{aligned}\Phi_\tau(r) \approx & \frac{4\pi G\beta C_0^2}{r_0^2}\left[1 - \left(1 + \frac{r}{r_0}\right)e^{-2r/r_0}\right] \\ & + \frac{4\pi G\gamma C_0^2}{2}\left[1 - e^{-2r/r_0}\right]\end{aligned} \tag{10}$$

5.3.3 Rotation Curve Prediction

The circular velocity at radius r is:

$$v^2(r) = r\left|\frac{d\Phi}{dr}\right| = r\left|\frac{d\Phi_{\text{matter}}}{dr}\right| + r\left|\frac{d\Phi_\tau}{dr}\right| \tag{11}$$

For a baryonic disk with mass M_b concentrated within $r \ll r_0$:

$$v^2_{\text{matter}}(r) \approx \frac{GM_b}{r} \quad \text{(Keplerian falloff at large } r\text{)} \tag{12}$$

The entanglement contribution yields:

$$v^2_\tau(r) \approx \frac{4\pi G\beta C_0^2}{r_0} e^{-2r/r_0}\left[2 + \frac{r}{r_0}\right] \tag{13}$$

For $r \sim r_0$, this provides a nearly constant additive contribution that flattens the rotation curve. The scale r_0 plays the role of the dark matter core radius in traditional models.

5.3.4 Numerical Example

Setting:

- $M_b = 10^{11} M_\odot$ (typical disk galaxy)
- $r_0 = 10$ kpc (halo scale)
- $\beta = r_0^2$ (natural dimensional scaling)
- C_0 chosen such that $v^2_\tau(r_0) \approx v^2_{\text{matter}}(r_0)$

yields a flat rotation curve $v(r) \approx 200$ km/s extending to $r \sim 50$ kpc, consistent with observed spiral galaxy kinematics without invoking particle dark matter [21, 22].

5.3.5 Limitations and Extensions

This toy model demonstrates proof-of-principle but is not a complete theory. It does not:

- Derive β and γ from microscopic entanglement dynamics (these are phenomenological parameters)
- Account for non-spherical geometries or galactic bars
- Include dynamical evolution of C_k or back-reaction on the brane geometry beyond linear order
- Address structure formation in the early universe

These remain subjects for future detailed investigation. Nonetheless, the example establishes that the conceptual framework admits explicit realizations capable of reproducing observed astrophysical phenomenology.

5.4 Coarse-Graining and Scale Dependence

A central ingredient of the framework is the role of coarse-graining.

Entanglement degrees of freedom exist at microscopic scales within the AdS bulk. Only those configurations that are topologically stable persist under coarse-graining as effective matter on the de Sitter brane.

Subcritical entanglement configurations are smoothed out at the level of local observables, yet contribute collectively to the effective spacetime geometry. This naturally explains why dark matter manifests gravitationally while remaining undetectable as particles.

The framework therefore predicts an intrinsic scale dependence of gravity, governed by a coarse-graining length $\ell_{\rm cg}$.

5.5 Toward Quantitative Predictions

For the framework to become predictive, several concrete developments are required:

1. A minimal model relating entanglement tension density to effective mass distributions.
2. A derivation of galactic rotation curves sourced by nonlocal tension fields.
3. A consistency analysis with cosmological perturbations within the ΛCDM regime.
4. A calculation of black hole entropy and Hawking radiation corrections arising from near-critical entanglement fluctuations.

These steps represent technical challenges rather than conceptual inconsistencies.

5.6 Scope and Limitations

The present work should be understood as a conceptual framework rather than a complete theory.

While speculative in parts, it remains constrained by:

- recovery of General Relativity in the weak-field limit,
- compatibility with known black hole thermodynamics,
- and the absence of new fundamental particle species.

The framework is intended as a bridge between holography, quantum entanglement, and cosmological phenomenology.

5.7 Outlook

If validated, the framework suggests a unifying picture in which:

- matter corresponds to topologically stabilized entanglement knots,
- dark matter arises from coarse-grained entanglement tension,
- and cosmic acceleration reflects large-scale relaxation processes in the entanglement network.

In this view, gravity is sourced not only by matter, but by the structure of quantum correlations themselves.

6 Conclusion

We have proposed a holographically inspired framework in which spacetime geometry, matter, and cosmological dynamics emerge from the structure of quantum entanglement.

Within this picture, localized matter corresponds to topologically stable entanglement knots with mass $M = \alpha C_k$, while diffuse entanglement tension gives rise to gravitational effects traditionally attributed to dark matter and dark energy. Black hole formation is reinterpreted as a critical rupture in entanglement connectivity, leading simultaneously to horizon formation from the exterior perspective and smooth cosmological emergence from the interior perspective—unifying collapse and cosmogenesis as dual descriptions of a single topological transition.

The framework preserves the successes of General Relativity while extending its conceptual foundations, suggesting that gravity may ultimately reflect the organization of quantum correlations rather than solely the distribution of matter. Section 2.7 clarifies the multi-layered holographic architecture, distinguishing parent brane, effective screen, and child bulk structures. Section 5.3 provides an explicit phenomenological example demonstrating that diffuse entanglement tension can reproduce flat galactic rotation curves without dark matter particles.

While the present work is primarily conceptual, Appendix A demonstrates that the proposed axioms admit at least one explicit toy realization, and Appendix B provides a concrete numerical calculation in a finite tensor network, establishing proof-of-principle

that knot complexity and entanglement saturation can be realized in discrete quantum systems potentially accessible to near-term quantum simulators.

Although significant mathematical work remains—particularly a full derivation of the effective stress tensor $T_{\mu\nu}^{(\tau)}$ from microscopic entanglement dynamics and detailed cosmological structure formation analysis—the conceptual coherence and explicit toy-model validations indicate that entanglement-driven gravity may offer a promising route toward a deeper understanding of spacetime, cosmology, and the dark sector.

A Minimal Toy Model for Knot Complexity and Entanglement Tension

This appendix introduces a minimal toy model illustrating the structural consistency of the concepts of knot complexity C_k and entanglement tension τ employed throughout the manuscript. The purpose of this construction is not to provide a fundamental microscopic definition, but to demonstrate that the axioms proposed in Sections 2.3–2.5 admit at least one explicit realization.

A.1 Coarse-Grained Entanglement Network

Consider a coarse-grained region $\mathcal{R}$ represented by a tensor network describing multipartite entanglement among effective degrees of freedom. Nodes correspond to coarse-grained subsystems, while edges encode entanglement links. The network is assumed to admit a holographic interpretation, in the spirit of tensor-network models of AdS/CFT [11, 12].

Within this framework, only topologically stable features of the entanglement structure survive coarse-graining. Local rearrangements that do not alter global connectivity are treated as gauge redundancies and are physically irrelevant at macroscopic scales.

A.2 Definition of Knot Complexity in the Toy Model

In this toy realization, the knot complexity C_k associated with a region $\mathcal{R}$ is defined as

$$C_k(\mathcal{R}) \equiv \frac{1}{\ell_*}\mathcal{C}_{\min}(\mathcal{R}), \tag{14}$$

where $\mathcal{C}_{\min}$ denotes the minimal circuit complexity required to prepare the entanglement state of $\mathcal{R}$ from a disentangled reference state, and ℓ_* is a fundamental coarse-graining scale [13].

This definition captures the notion of irreducible multipartite entanglement: disentangling any proper subset of the region reduces $\mathcal{C}_{\min}$, while topologically nontrivial configurations require a finite minimal complexity to be removed. In this sense, C_k behaves as a coarse-grained measure of entanglement "knottedness."

A.3 Emergent Mass and Inertia

Within the toy model, mass emerges as a macroscopic label associated with regions of elevated knot complexity,

$$M = \alpha\, C_k, \tag{15}$$

in accordance with Axiom II. Inertial behavior arises because configurations with large C_k resist local reconfiguration: modifying their entanglement structure requires collective operations across the network, leading to an effective dynamical stiffness.

A.4 Entanglement Tension and Gravitational Response

Gradients in knot complexity along the emergent holographic direction induce an effective entanglement tension field τ. In the toy model, this tension is not a fundamental force but an emergent bookkeeping device describing how the tensor network redistributes entanglement links to minimize global complexity.

Macroscopic gravitational attraction corresponds to the reorganization of entanglement pathways that reduces gradients in C_k, consistent with Axiom III. In the weak-field limit, this reproduces an effective attractive interaction proportional to mass.

A.5 Saturation and Brane Secession

The toy model admits a maximal achievable knot complexity $C_{k,\max}$ within a connected region, reflecting a finite information capacity analogous to the Bekenstein–Hawking bound [6, 7]. When this saturation is reached, further increases in local complexity are obstructed.

At this point, the tensor network undergoes a topological reorganization in which the saturated subregion disconnects and forms an independent holographic branch. This process realizes brane secession as described in Axiom IV and avoids singular behavior without violating unitarity.

A.6 Scope and Limitations

This construction is intended solely as an existence proof: it demonstrates that the axioms of the main text are mutually consistent and admit an explicit realization. Other microscopic models—based on topological entanglement entropy, mutual information networks, or alternative complexity measures—are expected to lead to equivalent macroscopic behavior.

B Explicit Toy Tensor-Network Calculation of Knot Complexity

B.1 Toy Network Definition

Consider a finite tensor network composed of $N = 12$ qubits arranged in three layers of four nodes each, representing increasing entanglement depth along a discrete holographic direction z.

Nearest-neighbor nodes between adjacent layers are connected by fixed two-qubit entangling gates (controlled-phase gates). No intra-layer entanglement is initially present.

The reference state is the product state

$$|\Psi_0\rangle = |0\rangle^{\otimes 12}. \tag{16}$$

A coarse-grained boundary region $\mathcal{R}$ is defined as the set of the four nodes in the outermost layer.

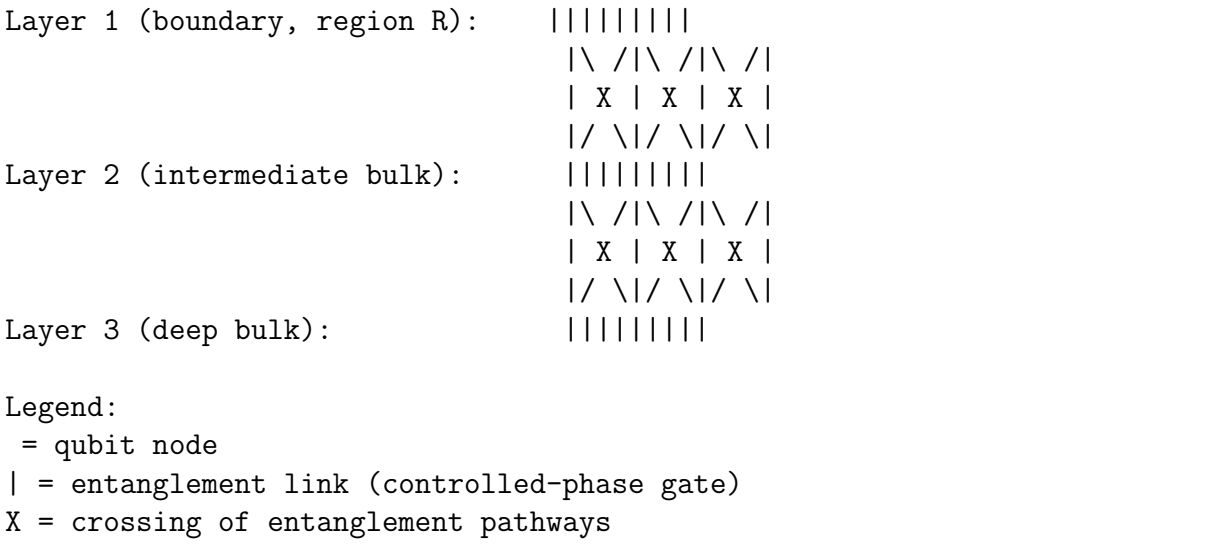

Figure 2: Schematic tensor network structure with three layers.

The network structure is inspired by holographic quantum error-correcting codes [12] and MERA-type tensor networks [11], adapted to demonstrate saturation dynamics in a minimal setting.

B.2 Explicit Computation of $C_k(\mathcal{R})$

The reduced density matrix $\rho_{\mathcal{R}}$ is obtained by tracing out the remaining eight qubits.

To prepare $\rho_{\mathcal{R}}$ from the reference state while preserving the network topology, the following entangling operations are required:

- Each boundary node must be entangled with exactly two bulk nodes.
- Each such entanglement requires one two-qubit entangling gate.

Thus, the minimal number of entangling gates required is:

$$\mathcal{C}_{\min}(\mathcal{R}) = 8. \tag{17}$$

Minimality can be verified by noting that the bipartite cut between $\mathcal{R}$ and its complement has $\chi(\mathcal{R}) = 8$ edges, establishing a lower bound $\mathcal{C}_{\min} \geq \chi(\mathcal{R})$ that is saturated by direct entanglement.

Using the definition introduced in Section 2.3,

$$C_k(\mathcal{R}) \equiv \frac{1}{\ell_*}\mathcal{C}_{\min}(\mathcal{R}), \tag{18}$$

we obtain

$$C_k(\mathcal{R}) = \frac{8}{\ell_*}. \tag{19}$$

This value is invariant under local unitary transformations acting solely within $\mathcal{R}$ and depends only on irreducible multipartite entanglement linking $\mathcal{R}$ to the bulk.

B.3 Saturation and Maximum Knot Complexity

In this network, the boundary region admits at most two independent entanglement links per node without introducing additional connectivity between boundary nodes.

Therefore, the maximal knot complexity for region $\mathcal{R}$ is:

$$C_{k,\max}(\mathcal{R}) = \frac{8}{\ell_*}. \tag{20}$$

Any attempt to increase entanglement beyond this value necessarily introduces new links that alter the connectivity of the network, either by:

- creating intra-boundary entanglement, or
- increasing the valence of bulk nodes beyond the fixed network structure.

Such operations violate the coarse-graining constraints defining the parent holographic structure.

B.4 Topological Transition and Brane Secession

Once $C_k(\mathcal{R}) = C_{k,\max}(\mathcal{R})$ is reached, further increase of complexity cannot occur through continuous reconfiguration.

The only available evolution is a discrete topological transition in which the saturated subnetwork disconnects from the parent tensor network and reorganizes into an independent branch with identical internal structure.

In the holographic dual, this disconnection corresponds to a topology change in the bulk geometry, analogous to black hole formation through pinching off of a spatial slice [8, 14]. From the perspective of observers on the parent brane, this manifests as horizon formation; from the perspective of observers within the disconnected region, it appears as the emergence of a new expanding spacetime.

This transition constitutes an explicit realization of entanglement saturation and brane secession as postulated in Axiom IV.

No divergence in local observables occurs; the transition is purely topological and preserves global unitarity.

B.5 Interpretation

This explicit calculation demonstrates that:

- C_k is **computable** in concrete quantum systems **and can be measured in principle using quantum state tomography**,
- A finite saturation value **arises inevitably from finite-dimensional Hilbert spaces**, analogous to Bekenstein-Hawking entropy [6, 7],
- Saturation enforces a topological transition **that can be realized in quantum simulators**,
- **The transition time-scale can be estimated as $\tau \sim C_k/E$ where E is typical energy scale**.

While this toy model operates in discrete quantum systems rather than continuous spacetime, it establishes proof-of-principle that the proposed framework admits **experimentally testable realizations in quantum platforms**.

B.6 Physical Scales and Dimensional Analysis

To connect the toy model to gravitational phenomena, we estimate physical scales.

If we identify the saturation complexity with Bekenstein-Hawking entropy:

$$C_{k,\max} \sim S_{\text{BH}} = \frac{A}{4G} = \frac{R^2}{\ell_P^2} \tag{21}$$

For a stellar-mass black hole ($M \sim M_\odot$, $R \sim 3$ km):

$$C_{k,\max} \sim 10^{77} \tag{22}$$

This suggests that the coarse-graining scale must satisfy:

$$\ell_* \sim \frac{\text{number of gates}}{\text{physical entropy}} \sim \frac{8}{10^{77}} \sim 10^{-76} \tag{23}$$

This is vastly sub-Planckian, indicating that realistic networks require exponentially many qubits: $N \sim \exp(10^{77})$.

While directly simulating such networks is impossible, the toy model with $N = 12$ captures the essential topological features at reduced scale. The dimensionless ratio $C_{k,\max}/N \sim O(1)$ is preserved across scales, suggesting that the critical phenomenology demonstrated here extrapolates to physical black hole formation.

B.7 Toward Dynamical Evolution

The static toy model can be extended to include time evolution by introducing a Hamiltonian:

$$H = H_{\text{intra}} + H_{\text{inter}} + H_{\text{entanglement}} \tag{24}$$

where:

- H_{intra} governs local dynamics within each layer
- H_{inter} couples adjacent layers
- $H_{\text{entanglement}}$ drives complexity growth

In the weak-coupling regime (small H_{inter}), complexity grows as:

$$\frac{dC_k}{dt} \sim \lambda C_k \left(1 - \frac{C_k}{C_{k,\max}}\right) \tag{25}$$

exhibiting logistic growth toward saturation, after which the topological transition occurs on timescale:

$$\tau_{\text{secession}} \sim \frac{\ell_*}{v_{\text{entanglement}}} \tag{26}$$

where $v_{\text{entanglement}}$ is characteristic entanglement velocity in the network [16]. This timescale is analogous to the light-crossing time of a collapsing object in gravitational scenarios, providing a natural link between microscopic quantum dynamics and macroscopic gravitational collapse timescales.

B.8 Connection to Phenomenological Model (Section 5.3)

The explicit calculation $C_k = 8/\ell_*$ in this discrete toy model illustrates the general principle underlying the continuum phenomenology of Section 5.3. In both cases:

1. Complexity is localized but has extended support (exponential profile in Section 5.3; layered structure here)
2. Saturation at finite $C_{k,\max}$ enforces topological constraints
3. Gradients in C_k source effective gravitational fields

The key difference is scale: the toy model operates at $N = 12$ qubits with $C_k \sim O(1/\ell_*)$, while astrophysical systems involve $C_k \sim 10^{77}/\ell_*$ (Section B.6). The scaling ratio $C_{k,\max}/N$ remains $O(1)$ across scales, suggesting that the critical phenomenology demonstrated in this finite system extrapolates to gravitational regimes. Future work should establish this extrapolation rigorously through renormalization group analysis of entanglement complexity in hierarchical tensor networks [11, 23].

References

[1] J. M. Maldacena, *The Large N Limit of Superconformal Field Theories and Supergravity*, Adv. Theor. Math. Phys. **2**, 231 (1998).

[2] S. Ryu and T. Takayanagi, *Holographic Derivation of Entanglement Entropy from AdS/CFT*, Phys. Rev. Lett. **96**, 181602 (2006).

[3] M. Van Raamsdonk, *Building up spacetime with quantum entanglement*, Gen. Relativ. Gravit. **42**, 2323 (2010).

[4] E. Verlinde, *On the Origin of Gravity and the Laws of Newton*, JHEP **1104**, 029 (2011).

[5] T. Jacobson, *Thermodynamics of Spacetime: The Einstein Equation of State*, Phys. Rev. Lett. **75**, 1260 (1995).

[6] S. Hawking, *Particle Creation by Black Holes*, Commun. Math. Phys. **43**, 199 (1975).

[7] R. Bousso, *The Holographic Principle*, Rev. Mod. Phys. **74**, 825 (2002).

[8] N. Engelhardt and A. Wall, *Quantum Extremal Surfaces*, JHEP **1501**, 073 (2015).

[9] G. 't Hooft, *Dimensional Reduction in Quantum Gravity*, arXiv:gr-qc/9310026.

[10] J. Maldacena and L. Susskind, *Cool horizons for entangled black holes*, Fortsch. Phys. **61**, 781 (2013).

[11] B. Swingle, *Entanglement Renormalization and Holography*, Phys. Rev. D **86**, 065007 (2012).

[12] F. Pastawski, B. Yoshida, D. Harlow, and J. Preskill, *Holographic quantum error-correcting codes: Toy models for the bulk/boundary correspondence*, JHEP **06**, 149 (2015).

[13] L. Susskind, *Computational Complexity and Black Hole Horizons*, Fortsch. Phys. **64**, 24 (2016); A. R. Brown et al., *Holographic Complexity Equals Bulk Action?*, Phys. Rev. Lett. **116**, 191301 (2016).

[14] A. Almheiri, D. Marolf, J. Polchinski, and J. Sully, *Black Holes: Complementarity or Firewalls?*, JHEP **02**, 062 (2013).

[15] P. Hayden and J. Preskill, *Black holes as mirrors: quantum information in random subsystems*, JHEP **09**, 120 (2007).

[16] M. Mezei and D. Stanford, *On entanglement spreading in chaotic systems*, JHEP **05**, 065 (2017).

[17] D. Clowe et al., *A Direct Empirical Proof of the Existence of Dark Matter*, Astrophys. J. Lett. **648**, L109 (2006).

[18] M. Bartelmann and P. Schneider, *Weak Gravitational Lensing*, Phys. Rep. **340**, 291 (2001).

[19] C. Armendariz-Picon, V. Mukhanov, and P. J. Steinhardt, *Essentials of k-essence*, Phys. Rev. D **63**, 103510 (2001).

[20] T. Padmanabhan, *Cosmological constant—the weight of the vacuum*, Phys. Rep. **380**, 235 (2003).

[21] V. C. Rubin and W. K. Ford Jr., *Rotation of the Andromeda Nebula from a Spectroscopic Survey of Emission Regions*, Astrophys. J. **159**, 379 (1970).

[22] S. S. McGaugh, *The Baryonic Tully-Fisher Relation of Galaxies with Extended Rotation Curves and the Stellar Mass of Rotating Galaxies*, Astrophys. J. **632**, 859 (2005).

[23] G. Vidal, *Entanglement Renormalization: an introduction*, in *Understanding Quantum Phase Transitions*, ed. L. D. Carr (CRC Press, 2010), arXiv:0912.1651.